Tu-AM-I7

RAMAN SPECTROSCOPY OF LIGAND BINDING TO MYOGLOBIN AT HIGH PRESSURE. ((A. Schulte, C. Williams)) Department of Physics and Center for Research in Electro-Optics and Lasers, University of Central Florida, Orlando, FL 32817.

The effect of high pressure on the resonance Raman spectrum of (horse) carbonmonoxymyoglobin was measured using excitation at 457 nm. By monitoring the oxidation state marker bands (ν_4 : 1374 cm^{-1} for MbCO and 1356 cm^{-1} for Mb) we show that there is a significant increase of the band at 1374 cm^{-1} relative to that at 1356 cm^{-1} upon raising the pressure from 1 atm to 180 MPa. This is consistent with a negative activation volume of MbCO. We explore conformational transitions of the protein by performing experiments with cyclic pressure changes.

* Supported by NSF, Grant No. MCB-9305711.

Tu-AM-I8

MULTI-VARIABLE APPROACH TO THE DESIGN OF CROSSLINKED HEMOGLOBINS ((Kenneth W. Olsen, Liang Zhao, Yaguo Zheng, Mary F. Reifsteck, Frank L. White and K. Sujatha)) Department of Chemistry, Loyola University, 6525 N. Sheridan Rd., Chicago, IL 60626.

Computer-aided molecular design is being used to propose new crosslinking reagents for human hemoglobin. In this design process, molecular dynamics calculations have been used to assess the flexibility of both the reagent and the reaction site on the protein. Long, hydrophilic diaspirin reagents have been designed to crosslink different hemoglobin tetramers together or to crosslink hemoglobin to protective enzymes, such as catalase or superoxide dismutase. Multilinkers, which react with the protein at more than two sites, are being made to modify single hemoglobin tetramers and to form hemoglobin octamers. Reagents designed to react between tetramers as they are oriented in the crystalline state are also being used. These reagents offer the possibility of forming complexes that cannot be made in solution. Finally, molecular dynamics simulations are being used to predict the effects of crosslinking on protein flexibility. (Supported in part by a grant from the Research Corporation.)

Tu-AM-I9

FLUORINATED IRON DODECAPHENYLPORPHYRINS AS ALKANE-OXIDATION CATALYSTS. ((M. C. Showalter, K. E. Erkkila, J. A. Shelnutt)) *Fuel Science Department 6211, Sandia National Laboratories, Albuquerque, NM 87185-5800.*

Computer-aided molecular design methods are being used in conjunction with catalytic activity testing to develop biomimetic iron-porphyrin catalysts that incorporate the structural features responsible for enzyme catalysis. In this work the focus is on models of cyctochromes P450. A series of fluorinated iron dodecaphenyporphyrins ($FeDPPF_x$, where x = 0, 20, 28, and 36) has been synthesized, characterized, and tested for catalytic activity. Desired molecular design features in these catalysts include a substrate binding cavity common to the entire series and increased electron-withdrawing ability of the porphyrin ligand across the series as the number of fluorine substituents increases. These porphyrins were tested as catalysts in the oxidation of light alkanes, including isopentane, to alcohols. Catalytic activity was found to increase with the number of fluorine substituents regardless of whether iodosylbenzene or O_2 was used as the oxidant. This increase in activity is attributed solely to the electronic effect of the fluorine substituents because molecular modeling and spectroscopic studies show that replacing hydrogen with fluorine on the phenyl substituents does not alter the conformation of the porphyrin macrocycle. In addition, these catalysts, which have a substrate binding cavity, show novel selectivities in some reactions. Future work will involve using the insights gained thus far to continue designing catalysts which are predicted to be more active and selective.

Supported by United States Department of Energy Contract DE-AC04-94AL85000.

SEVEN HELIX RECEPTORS

Tu-PM-Sym-1

CONSTITUTIVE ACTIVATION OF RHODOPSIN AS A MOLECULAR MECHANISM OF DISEASE. ((D.D. Oprian)) Dept. of Biochemistry, Brandeis University, Waltham, MA 02254.

We have identified four different amino acid residues in the visual pigment rhodopsin that when mutated cause constitutive activation of the apoprotein opsin. These amino acids are Gly^{90}, Glu^{113}, Ala^{292}, and Lys^{296}. In each case, activation of the mutant protein appears to result from the disruption of a salt bridge between Glu^{113} and Lys^{296}. Mutations at three of these positions ($Gly^{90} \rightarrow$ Asp, $Ala^{292} \rightarrow$ Glu, and $Lys^{296} \rightarrow$ Glu or Met) have been found in the diseases congenital night blindness and retinitis pigmentosa. We speculate that the unregulated activity of the mutant receptors is causing disease in patients with these mutations. We are currently designing active site-directed inactivators which selectively target the constitutively active mutant receptors.

Tu-PM-Sym-2

LIGAND BINDING DOMAINS OF G PROTEIN COUPLED RECEPTORS. ((C.D. Strader, T.M. Fong, M.R. Candelore, and M.R. Tota)) Merck Research Labs, Rahway, NJ 07065.

Receptors whose mechanism of action is mediated through the activation of G proteins share structural, as well as functional, similarities. These receptors consist of seven hydrophobic domains, postulated to form transmembrane helices, connected by hydrophilic loops. Site-directed mutagenesis of the ß-adrenergic receptor has shown that the ligand binding domain is contained within the transmembrane core of the receptor, with most of the binding energy provided by an ion pair formed between the amine group of the catecholamine ligand and the carboxylate side chain of Asp113 in the third transmembrane domain of the receptor. G protein activation is triggered by interactions of the catechol ring of the ligand with residues in helices 5 and 6 of the receptor. In contrast to the relatively compact ligand binding domain of the catecholamine receptors, the undecapeptide substance P binds to both the transmembrane and extracellular regions of the NK1 neurokinin receptor. Small molecule antagonists of this receptor have recently been described, and specific interactions between these antagonists and residues in the transmembrane domain of the NK1 receptor have been identified. The similarity in the location of the non-peptide antagonist binding site in the NK1 receptor with that of the biogenic amine binding site in the ß-adrenergic receptor suggests the existance of a generally conserved binding site for small molecules in the transmembrane domains of G protein coupled receptors.

Tu-PM-Sym-3

THE STRUCTURE OF G PROTEIN-COUPLED RECEPTORS
((J.M. Baldwin)) MRC Laboratory of Molecular Biology, Hills Road, Cambridge CB2 2QH, UK.

All members of the family of G protein-coupled receptors are expected to have the same basic structure in the membrane-embedded part of the protein because they share distinctive sequence patterns in their seven hydrophobic segments and they have a common interaction with G-proteins. The probable arrangement of the seven helices in these receptors has been deduced from structural information extracted from a detailed analysis of their sequences. It has been established that helices I, IV and V are most exposed to the lipid surrounding the receptor and helix III is least exposed. Evidence for this comes from considering: (1) the sites of the most conserved residues; (2) the sites that accommodate polar residues; (3) the sites of differences in sequence between pairs or within groups of closely related receptors. Most sites in category (3) should be in unimportant positions and are most useful in determining the position and extent of the lipid-facing surface in each helix. Sites in categories (1) and (2) should face towards the inside of the molecule. It has also been established that each helix must be positioned next to its neighbours in the sequence. Evidence for this comes from considering the shortest length seen for each inter-segment loop in the whole family of sequences. The structural constraints for the receptors have been useful in allocating particular helices to peaks in the projection map of rhodopsin that has been determined by electron crystallography of 2-D crystals (Schertler et al. Nature 1993, 362:770-772). They will be even more useful in enabling model building from a three-dimensional map that might be obtainable only at relatively low resolution.

Tu-PM-Sym-4

MOLECULAR MECHANISMS OF ACTIVATION AND DESENSITIZATION OF G PROTEIN-COUPLED RECEPTORS.
((R.J. Lefkowitz)), HHMI, Duke University Medical Center, Durham, NC 27710.

The adrenergic receptors which are coupled to guanine nucleotide regulatory proteins have a characteristic seven membrane spanning domain topography. Activation of G proteins is carried out by sequences in the cytoplasmic domains of the receptor, especially those in close apposition to the plasma membrane. Mutations in the third cytoplasmic loop of several adrenergic receptors lead to constitutive activation, by changing receptor conformation to mimic the active state of the wild type receptor. The mutated region may function to constrain the G protein coupling of the receptor, a constraint which is normally relieved by agonist occupancy. Several disease states are caused by such mutations of other G protein-coupled receptors. The function of these receptors is controlled by phosphorylation reactions. Six members of a novel family of G protein-coupled receptor kinases have been cloned so far. These enzymes phosphorylate only the activated form of the receptors. Both rhodopsin kinase and βARK1 and 2 are cytosolic enzymes which translocate to the plasma membrane upon receptor activation. In the case of rhodopsin kinase, this requires farnesylation at its C terminus. In contrast, the βARKs are not prenylated but rather bind through specific sites on their carboxy termini to the prenylated βγ subunit complex of the heterotrimeric G proteins. This serves to target the kinases to the membrane bound receptor substrates. Peptides, the sequences of which are based on the βγ binding region of the kinases, block kinase translocation, receptor phosphorylation, and desensitization in various cellular systems. Moreover, they also block several other Gβγ-mediated effector actions in cells Such reagents may prove useful in dissecting the relative contributions of Gα and Gβγ subunits to activation of various cellular effectors.

SMOOTH MUSCLE BIOCHEMISTRY AND PHYSIOLOGY

Tu-PM-A1

PLASTICITY IN SMOOTH MUSCLE
((V.R. Pratusevich, C.Y. Seow, and L.E. Ford)) Dept. of Medicine, Univ. of Chicago, Chicago, IL 60637

The large volume changes of some hollow viscera (bowel, bladder, uterus) indicate a greater length range for the smooth muscle of their walls than can be accommodated by a fixed array of sliding filaments. The controversial findings that smooth muscle thick filaments can be evanescent suggest that these muscles adapt to length changes by forming variable numbers of contractile units in series. To test for such plasticity we examined the muscle length dependence of shortening velocity and compliance, both of which will vary directly with the number of thick filaments in series. Dog tracheal smooth muscle was studied because its cells are arrayed in long, straight, parallel bundles that span the length of the preparation. Over a 3-fold length range velocity varied 2.3-fold and compliance 1.9-fold while isometric force varied by less than 25%. This relative length independence of isometric force is only seen, however, when the muscle is conditioned to each new length. Tetanic force is initially depressed by length changes in either direction, and then increases to a steady level with 5-6 tetani at 5 min. intervals. These results suggest very strongly that the number of contractile units in series varies directly with the adapted muscle length. Temporary force depression following a length change would occur if the change transiently moved the filaments from their optimum overlap. The relative length-independence of the adapted force is explained by the reforming of the filament array to produce optimum force development, with commensurate changes of velocity and compliance.

Tu-PM-A2

REDUCED FORCE GENERATING CAPACITY IN SHORTENING CONTRACTION OF CANINE AIRWAY SMOOTH MUSCLE IS NOT DUE TO SHORTENING DEACTIVATION
((Weilong Li & Newman L. STEPHENS)) Dept. of Physiology, Univ. of Manitoba, Winnipeg, Manitoba, Canada R3E 0W3

Previous studies have shown that force generating capacity in afterloaded isotonic contraction is significantly reduced compared with that of isometric contraction at the same muscle length. A recognized explanation is that muscle shortening reduces contractility. If this hypothesis is correct, one would expect increased reduction of force generation with increased shortening. We tested the hypothesis by imposing on the activated muscle different shortening(ΔL) dependent loads(R) of the following characteristics: logarithmic $R = K \times Log(A \times \Delta L + 1)$, linear $R = K \times \Delta L$, sigmoidal $R = K \times EXP(A-B/\Delta L)$, exponential $R = EXP(\Delta L \times K)$, where K is the adjustable constant. Experiments were carried out by selecting different K values to obtain force-length relation for corresponding loading modes. We found that the muscle was able to develop greater shortening under exponential loading mode than under logarithmic even though the final force developed under the two loading modes was the same. We also found that the force-shortening plot for auxotonic contraction was identical to the load-shortening plot, suggesting the force generated is load-dependent and not muscle contractile element length-dependent. Based on the fact that shortening capacity of smooth muscle also varies as a function of activation time, we conclude that the reduced force-length relation is not due to shortening deactivation but to an inhibitory effect of the load on shortening occurring in the fist 2s of a contraction (70% of total shortening is completed at this time) whose total contraction time is 10 seconds (Supported by Medical Research Council of Canada, Weilong Li is the recipient of a studentship of Manitoba Health Research Council)

Tu-PM-A3

DISSOCIATION OF RELAXATION AND MYOSIN LIGHT CHAIN DEPHOSPHORYLATION IN SMOOTH MUSCLE.
((M. Bárány, L. Hegedüs and K. Bárány)) Depts. of Biochemistry, and Physiology and Biophysics, Col. of Med., Univ. of Illinois, Chicago, IL 60612.

Several laboratories have reported dissociation of smooth muscle relaxation and myosin light chain (MLC) dephosphorylation: in tracheal muscles (Gerthoffer, Am. J. Physiol. 250, C597, 1986; Tansey, et al., FEBS Lett. 270, 219, 1990; Katoch, Indian J. Exp. Biol. 30, 252, 1992) and in arterial muscles (McDaniel, et al., Am. J. Physiol. 263, C461, 1992; D'Angelo, et al., J. Clin. Invest. 89, 1988, 1992). Recently, we have shown that porcine uterus, a phasic muscle, contracted by carbachol, histamine, or oxytocin can be relaxed by Mg^{2+}, isoproterenol, or nitroprusside without a significant MLC dephosphorylation (Bárány and Bárány, Arch. Biochem. Biophys. 305, 202, 1993). We have studied the relationship between fractional MLC dephosphorylation and fractional relaxation in smooth muscles. Histamine contracted porcine carotid arterial muscles were relaxed to various extents by washings with physiological salt solution, isoproterenol, or Mg^{2+}, and carbachol contracted porcine bladder muscles were relaxed by Mg^{2+}. In these cases, MLC dephosphorylation lagged behind relaxation and complete dephosphorylation was observed only after the relaxation had been completed. It can be concluded that MLC dephosphorylation is not a prerequisite for smooth muscle relaxation. Accordingly, the contraction-relaxation cycle of smooth muscle cannot be explained by an exclusive MLC phosphorylation-dephosphorylation mechanism. (Supported by NIH, AR34602 and T32HL07692).

Tu-PM-A4

CALPONIN PHOSPHORYLATION DOES NOT ACCOMPANY CONTRACTION OF VARIOUS SMOOTH MUSCLES.
((K. Bárány and M. Bárány)) Depts. of Physiology and Biophysics, and Biochemistry, Col. of Med., Univ. of Illinois, Chicago, IL 60612.

The NEPHGE-SDS two-dimensional electrophoresis procedure of O'Farrell, et al. (Cell 12, 1133, 1977) was used for studying calponin phosphorylation during contraction of ^{32}P-labeled porcine smooth muscles from artery, uterus, trachea, stomach and bladder. Calponin phosphorylation could be detected when the gels were exposed to prolonged autoradiography, but with the long exposure time virtually all protein spots exhibited radioactivity. A new method was developed for measuring calponin concentration in smooth muscle. This allowed quantitation of calponin phosphorylation. In 36 smooth muscles analyzed, the extent of calponin phosphorylation was very low, it ranged from 0.002 to 0.010 moles [^{32}P]phosphate per mole calponin. There was no increase in calponin phosphorylation, above that in the resting muscle, when the five different smooth muscles were contracted by various agents for varying times. In the same contracting muscles, phosphorylation of myosin light chain (MLC) was increased 3.5-6.5-fold. The [^{32}P]phosphate content of MLC, 0.310-0.614 mol/mol, was 50-250-fold higher in the contracting muscle than that of calponin in the same muscle. NEPHGE-SDS resolved six spots of calponin without any change in the staining distribution between resting and contracting muscles. In contrast, changes in the staining distribution of the MLC spots were readily detectable on the same NEPHGE-SDS gels. The results indicate no involvement of calponin phosphorylation in smooth muscle contraction. (Supported by NIH, AR34602).

Tu-PM-A5

PHOSPHORYLATION OF MYOSIN LIGHT CHAIN KINASE IN SWINE CAROTID ARTERY. ((D.A.Van Riper, B. A. Weaver, and C. M. Rembold)) Cardiovascular Division (Internal Medicine), University of Virginia, Charlottesville, VA USA (sponsor N. McDaniel)

Phosphorylation of tracheal or gizzard myosin light chain kinase (MLCK) on the 'A' site decreases its affinity for Ca^{2+}-calmodulin. We investigated the role of MLCK phosphorylation in swine carotid artery. In vitro, the catalytic subunit of protein kinase A phosphorylated swine carotid MLCK on site 'B' in the absence of Ca^{2+} and on site 'A' and 'B' in the presence of Ca^{2+}. This identified the 'A' site as the phosphorylation site that regulates Ca^{2+}-sensitivity. In unstimulated swine carotid medial tissues pre-labeled with ^{32}P, there was substantial MLCK phosphorylation (0.65 ± 0.07 mol/mol), however, only 9.0 ± 3.5 % was at the 'A' site. Stimulation with 109 mM KCl increased MLCK phosphorylation (1.04 ± 0.08 mol/mol) primarily from an increase to 40.1 ± 4.0 % at the 'A' site. There was an inverse relation between MLCK phosphorylation at the 'A' site and the Ca^{2+}-sensitivity of MLCK activity measured in swine carotid extracts (activity ratio). In tissues treated with histamine, high $[K^+]_o$, or high $[K^+]_o$ & forskolin, MLCK phosphorylation and the Ca^{2+}-sensitivity of MLCK correlated with aequorin-estimated $[Ca^{2+}]_i$, suggesting that $[Ca^{2+}]_i$ is the primary determinant of MLCK phosphorylation. We are now investigating whether other stimuli can alter the relationship between $[Ca^{2+}]_i$ and MLCK phosphorylation. Support: NIH HL38918 & VA AHA.

Tu-PM-A6

INTERACTION BETWEEN CALPONIN AND SMOOTH MUSCLE MYOSIN. ((P.T. Szymanski and T. Tao)) Boston Biomedical Res. Inst., 20 Staniford St., Boston, MA 02114.

Calponin is a thin filament-associated protein in smooth muscle that has been implicated to play a role in regulation of smooth muscle contractility. It has been shown to bind actin, tropomyosin and calmodulin, and to inhibit actomyosin ATPase activity. We have used a centrifugation assay to examine whether calponin can interact with myosin directly. We found that calponin can bind to unphosphorylated, filamentous smooth muscle myosin, and that this binding is reversible by Ca^{2+}-CaM. The strength of the calponin-myosin interaction depends on NaCl concentration, being relatively strong at 50 mM NaCl and virtually undetectable at 150 mM NaCl. The binding constant between calponin and myosin is approximately 2 x 10^6 M^{-1} at 50 mM NaCl, and the stoichiometry of this interaction is in the range of 1.2-2.4 calponin per myosin. Our results suggest that calponin can bind to myosin as well as to actin, so that it may play a role in regulation of smooth muscle contractility by anchoring the two proteins. (Supported by NIH P01-AR41637 and AHA).

Tu-PM-A7

MODULATION OF MITOGEN-ACTIVATED PROTEIN KINASE ACTIVITY AND CONTRACTILITY IN PORCINE CAROTID ARTERIES. ((L.P. Adam, G. Raff and D.R. Hathaway)) Krannert Institute of Cardiology, Indiana University, Indianapolis, Indiana.

h-Caldesmon (M_W=93,000) is a potent modulator of actomyosin activity in vitro and may, therefore, be regulatory for contraction in intact tissue. h-Caldesmon is phosphorylated in response to pharmacologic stimulation and the sites phosphorylated in intact tissue are identical to the sites phosphorylated by mitogen-activated protein kinase (MAPK), in vitro. In order to assess a role for this kinase in contractile activation, a peptide substrate (APRTPGGRR) was used to measure MAPK activity in unstimulated porcine carotid arteries and in arteries stimulated with either KCl or phorbol-12,13-dibutyrate (PDBu). Fractionation of tissue extracts by Mono-Q chromatography separated two peaks of kinase activity corresponding to the two MAPK isoforms: $p42^{MAPK}$ and $p44^{MAPK}$. Activity associated with $p42^{MAPK}$ accounted for 37% of the total; this percentage was not altered by pharmacological stimulation of the muscles. Both MAPK isoforms could phosphorylate h-caldesmon, stoichiometrically, in vitro. The ratio of h-caldesmon phosphorylation by p42/p44 was similar to the ratio of activity towards the peptide substrate. Kinase activity in resting muscle, when assayed with the peptide substrate, was 126 pmole phosphate/min/mg protein. With KCl stimulation, the activity rose to a peak level of 211 at 10 min and then declined to near resting values at 30 min (159 pmole/min/mg protein). Stimulation by PDBu (1 μM) led to an increase in kinase activity that was maintained- 146, 183, and 201 pmole/min/mg protein at 10, 30 and 60 min of stimulation, respectively. These data show that a) MAPK is active in resting, contractile phenotype, vascular smooth muscle and b) this activity is enhanced by agents that contract the muscle. Activation of MAPK and the subsequent phosphorylation of h-caldesmon may modulate force maintenance in vascular smooth muscle.

Tu-PM-A8

SMOOTH MUSCLE TROPOMYOSIN ENHANCES THE COOPERATIVE ACTIVATION BY MYOSIN PHOSPHORYLATION OF ISOMETRIC FORCE PRODUCTION IN AN *IN VITRO* MOTILITY ASSAY. ((J.R. Haeberle)) Dept. of Molecular Physiology and Biophysics, The University of Vermont, Burlington, VT 05405.

It is well established that only 0.2-0.5 mol PO_4 per mol of myosin regulatory light chain (LC_{20}) is required for maximal isometric force production by vertebrate smooth muscles. To address the question of how unphosphorylated myosin is activated, an *in vitro* motility assay was used to evaluate the effects of LC_{20} phosphorylation on unloaded filament velocity and isometric-force production in the presence and absence of tropomyosin (Tm). Mixtures of monomeric (300 mM KCl) unphosphorylated (UPM) and thiophosphorylated (2.0 mol/mol, TPM) chicken gizzard smooth muscle myosin were bound to a nitrocellulose-coated coverslip. To measure relative isometric force production, isometric conditions were created by adding NEM-modified skeletal muscle myosin to the coverslip to mechanically load the filaments. The minimum amount of NEM-modified myosin required to stop actin-filament motion provided an index of relative isometric force (F_{NEM}). In the absence of Tm, activation of force production by TPM was cooperative (18% max F_{NEM} with 5% TPM, 57% max F_{NEM} with 20% TPM, and 100% max F_{NEM} with 100% TPM). Tm increased the max F_{NEM} by 68%, and greatly increased the cooperativity of activation (75% max F_{NEM} with 5% TPM, 78% max F_{NEM} with 20% TPM, and 100% max F_{NEM} with 100% TPM). In addition, force production by UPM was observed when actin•Tm filaments were predecorated with NEM-modified myosin (i.e. rigor-dependent activation). These results suggest that cooperative switching-on of the actin filaments by rigor cross bridges or by thiophosphorylated cross bridges, activates force production by unphosphorylated cross bridges. Unloaded filament velocity was constant at all levels of phosphorylation and unaffected by Tm, suggesting that the increased force could not be accounted for by a reduced rate of cross-bridge dissociation (i.e. latch-bridges).

Tu-PM-A9

CALDESMON DISRUPTS COOPERATIVE ACTIVATION OF UNPHOSPHORYLATED MYOSIN BY PHOSPHORYLATED SMOOTH MUSCLE MYOSIN ((M.E. Hemric, and J.R. Haeberle)) Dept of Molecular Physiology and Biophysics, University of Vermont, Burlington, VT 05405.

We have previously used the *in vitro* motility assay to measure the effect of caldesmon on unloaded actin filament velocity (Haeberle et al., (1992) J. Biol. Chem.267, 23001-23006). Relative isometric force can be measured in the assay by mixing NEM-modified skeletal muscle myosin with smooth muscle myosin to impose a mechanical load on the filaments. Using this method, Haeberle has demonstrated the cooperative activation of unphosphorylated smooth muscle myosin by phosphorylated smooth muscle myosin is dependent upon tropomyosin (abstract, this meeting). By inhibiting the binding of myosin to actin, caldesmon could reduce the cooperativity of activation by phosphorylated myosin. To test this hypothesis, the effect of caldesmon, and the actin-binding fragment of caldesmon, on isometric force was measured with varied ratios of thiophosphorylated to unphosphorylated smooth muscle myosins in the presence of smooth muscle tropomyosin. The addition of caldesmon or the actin-binding fragment of caldesmon reduced isometric force by 60% (20% thiophosphorylated myosin) and 15% (100% phosphorylated myosin), demonstrating a reduction in cooperative activation. Phosphorylation of caldesmon by its copurifying "caldesmon kinase" reversed the effects. These results suggest that the actin-binding domain of caldesmon disrupts cooperative activation of unphosphorylated smooth muscle myosin by phosphorylated smooth muscle myosin.

Tu-PM-A10

REGULATION OF ACTIN FILAMENT VELOCITY BY CALDESMON: THE EFFECT OF UNPHOSPHORYLATED MYOSIN **((K.Y. Horiuchi and S. Chacko)) Department of Pathobiology, University of Pennsylvania, Philadelphia, PA 19104.**

The effect of caldesmon on the movement of actin filament over myosin at different levels of light chain phosphorylation was investigated. Smooth muscle myosin at different levels of phosphorylation was obtained by mixing different proportions of fully phosphorylated (P) and unphosphorylated (UP) myosin in monomeric form, while keeping the total myosin concentration constant. The movement of fluorescently labeled actin filament over the myosin attached on the nitrocellulose-coated coverslip was tested. The average velocity of actin filament was 1.01±0.14 μm/sec at 30°C with P myosin. In the presence of caldesmon, actin filament was not bound on the myosin coated surface. On the other hand, tropomyosin-actin filament bound to myosin in the presence of caldesmon, and the velocity was unaffected by caldesmon as reported by Haeberle *et al.* (*JBC*, 267:23001, 1992). On raising the percentage of UP myosin, the velocity was not altered until the P myosin was lowered to around 10% in the absence of caldesmon. However, in the presence of caldesmon, the velocity began to decrease before the P myosin reached 10%. This change in velocity is presumably caused by the tethering of actin filaments to UP myosin, due to the interaction of N-terminal domain of caldesmon and S-2 region of UP myosin. A rise in the population of UP myosin, as observed during force maintenance (latch), may increase this tethering effect, resulting in a significant mechanical load and a diminution in the movement of actin filaments.

Tu-PM-B1

AMP-PNP DELAYS THE CLOSING OF CFTR Cl CHANNELS OPENED BY ATP.
((G. Nagel*, T.-C. Hwang, A.C. Nairn, & D.C. Gadsby)) Labs of Cardiac Membr. Physiol. & Neurosci Rockefeller Univ., New York, NY 10021 *present address: MPI Biophysik, D-60596 Frankfurt

Effects of the nonhydrolyzable ATP analogue, AMP-PNP, on CFTR Cl channels in guinea pig ventricular myocytes were studied by recording whole-cell currents (at 36°C) with wide-tipped, perfused pipettes and single-channel currents (at 25°C) in excised inside-out giant patches. Whole-cell Cl conductance activated by forskolin decayed rapidly after its removal ($t_{1/2}$ = 1.0±0.1 min, n=6). But, replacing the 2 mM pipette ATP with 1 mM AMP-PNP + 1 mM ATP, in the continued presence of forskolin, increased the activated Cl conductance two fold (2.1±0.1 at 0 mV, n=4) and slowed its deactivation ($t_{1/2}$ = 4.6±0.2 min, n=6). In the absence of forskolin, AMP-PNP plus ATP did not affect membrane conductance. In inside-out patches, Cl channels with CFTR characteristics were activated by phosphorylation with the catalytic subunit of protein kinase A (PKA) plus MgATP. Channel activity could persist for >15 min in the presence of ATP after washout of PKA, but disappeared promptly on withdrawal of ATP. The PKA-phosphorylated channels could be reopened by ATP or GTP, but by neither ADP nor AMP-PNP. Sudden exposure to ATP reopened the channels rapidly ($t_{1/2} \leq$1s), but they closed more slowly ($t_{1/2}$ ~5s) on washing out the ATP. However, application of AMP-PNP in the presence of ATP could stabilize the open state of the channels so that they then closed extremely slowly ($t_{1/2}$ ~7min) after removal of both ATP and AMP-PNP. This slow closing cannot be attributed to irreversible rundown or complete dephosphorylation of the channels because brief applications of ATP opened the channels again. The slow closing presumably reflects the slow dissociation of AMP-PNP from a site on the channel. We can draw three tentative conclusions. First, CFTR must comprise two functionally distinct nucleotide binding sites. ATP or another hydrolyzable nucleoside triphosphate, but not AMP-PNP (nor ADP), can act at one of those sites to open a PKA-phosphorylated channel, presumably via a reaction involving hydrolysis, once a channel has been opened by ATP. AMP-PNP (and likely ATP too) can act at the other site to stabilize the open state. Second, because the principal difference between ATP and AMP-PNP is the stability of the latter's γ-phosphate, the greatly prolonged half life of AMP-PNP-bound channels relative to that of ATP-bound channels suggests that ATP hydrolysis also occurs at the other nucleotide binding site. Third, because AMP-PNP can act at one of the sites only after the channel has been opened by ATP acting at the other, there must be some functional interaction between the two nucleotide binding sites.
Supported by NIH, NYHA, and the CF Foundation.

Tu-PM-B2

DIFFERENTIAL REGULATION OF NUCLEOTIDE BINDING SITES IN CFTR BY PKA PHOSPHORYLATION. ((T.-C. Hwang, G. Nagel, A.C. Nairn, & D.C. Gadsby)) Laboratories of Cardiac/Membrane Physiology and Molecular and Cellular Neuroscience, The Rockefeller University, New York, NY 10021.

Deactivation of the whole-cell Cl conductance after washout of isoproterenol or forskolin becomes incomplete when type 1 and 2A cellular phosphatases are inhibited with maximally effective concentrations of okadaic acid (10 μM) or microcystin (10 μM). The smaller amplitude of the residual Cl coductance (~30% relative to the more fully activated Cl conductance) appears to reflect a lower open probability (P_o) of the partially phosphorylated channels. This residual Cl conductance was abolished by complete replacement of pipette ATP (2 mM) with equal concentration of AMP-PNP, suggesting that these partially phosphorylated Cl channels in intact myocytes, like PKA-phosphorylated CFTR Cl channels in excised patches, require hydrolyzable nucleoside triphosphate to stay open. On the other hand, replacement of only half the pipette ATP with AMP-PNP was entirely without effect on the residual Cl conductance in the presence of okadaic acid. Nevertheless, subsequent stimulation of PKA activated a somewhat larger than normal Cl conductance that decayed slowly ($t_{1/2}$ = 4.6±0.2 min, n=6). In excised inside-out membrane patches, unitary current measurements from a single CFTR molecule demonstrate both a sudden increase in P_o, from a lower (~0.2) to a higher level (~0.7), during channel activation by PKA-mediated phosphorylation, as well as a reduction of P_o after withdrawal of PKA that could be temporarily reversed by a brief re-exposure to PKA. These results suggest that the P_o of single CFTR Cl channels depends on the degree of their phosphorylation by PKA. When AMP-PNP was tested on partially dephosphorylated channels, with low P_o, in none of the five patches examined did AMP-PNP induce prolonged channel openings. In one of the patches (P_o = 0.13), complete replacement of ATP with AMP-PNP promptly closed all channels and, in the other four patches (P_o = 0.20±0.02), switches from 0.5 mM ATP to a mixture of 0.25 mM ATP plus 0.25 mM AMP-PNP failed to increase P_o. These results suggest that incremental phosphorylation of CFTR molecules affects Cl channel activity by differentially controlling the availability of two nucleotide binding sites, and that both nucleotide binding sites are required for optimal channel activity.
Supported by NIH, NYHA and the CF Foundation.

Tu-PM-B3

OPENING OF CFTR Cl CHANNELS IS COUPLED TO ATP HYDROLYSIS.
((T. Baukrowitz, T.-C. Hwang, A. C. Nairn, & D. C. Gadsby)) Laboratories of Cardiac/Membrane Physiology, and Molecular and Cellular Neuroscience, The Rockefeller University, New York, NY 10021.

The inorganic phosphate analogues orthovanadate (VO_4) and BeF_3 are well known to arrest ATPases by entering the cycle following ATP hydrolysis and binding in place of the dissociated phosphate to form a stable complex. We tested their influence on the gating of CFTR Cl channels, phosphorylated by PKA catalytic subunit, in giant patches excised from guinea pig ventricular myocytes. VO_4 (1-5 mM) had no effect on closed CFTR Cl channels but, in the presence of 0.5-1 mM MgATP, the channel open state was dramatically stabilized by VO_4 or BeF_3 (0.5 mM $BeSO_4$ + 5 mM CsF). The channels closed with a rate of roughly 2 s^{-1} when ATP was washed away in the absence of these analogues, but which was reduced to ~0.005 s^{-1} (VO_4) or ~0.002 s^{-1} (BeF_3), respectively, when a phosphate analogue accompanied the ATP. This effect could not have reflected phosphatase inhibition, because VO_4 could "lock" channels open long after (>10 min) withdrawal of PKA. Dwell times of channels in the locked-open state were exponentially distributed, were independent of the VO_4 concentration used to induce locking, and appeared independent of the subsequent presence or absence of VO_4. Analysis of the rate at which channels were locked open by VO_4 suggested that locking occurs only from the open state: the probability of a channel entering the locked state was directly proportional to the cumulative duration of open-state dwell times, and approximately independent of the channels' open probability before locking. The locking rate estimated in this way varied linearly with [VO_4] between 1 and 5 mM, yielding an apparent association rate constant for VO_4 of ~11 $M^{-1}s^{-1}$. As a phosphate analogue, VO_4 can interact with ATPases only after hydrolysis of ATP to ADP plus phosphate, and after dissociation of the phosphate. We therefore conclude that channel opening is coupled to an ATP hydrolysis cycle.
Supported by NIH, NYHA and the CF Foundation.

Tu-PM-B4

MOLECULAR AND ELECTROPHYSIOLOGICAL CHARACTERIZATION OF $CFTR_{cardiac}$ IN NORMAL AND CF HUMAN HEARTS. ((P. Hart, Y. Geary, J. Warth, M.L. Collier, T. Chapman, J.R. Hume, and B. Horowitz)) Department of Physiology, University of Nevada, Reno, NV 89557-0046. (Spon. by J. Peacock).

We have previously determined that the cAMP dependent Cl^- conductance in heart is due to cardiac expression of CFTR and that CFTR expressed in heart ($CFTR_{cardiac}$) is an alternatively spliced isoform of the epithelial gene product (Am. J. Physiol. 264:H2214, 1993). Much previous work on $CFTR_{cardiac}$ has been conducted on species other than human (rabbit, canine, guinea pig). In order to determine the relationship between CF mutations and $CFTR_{cardiac}$ we examined the molecular and electrophysiological nature of $CFTR_{cardiac}$ expressed in human heart. For molecular characterization, mRNA was prepared from normal human atria obtained from bypass patients and CF derived atria and ventricular tissue obtained post-mortem from CF patients. RT-PCR was performed on the mRNA employing the primers decribed in the figure.

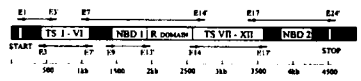

Primers E3 and E7' generated the alternatively spliced region of $CFTR_{cardiac}$ demonstrating that this form of CFTR is expressed in human atrium and ventricle. Analysis of the NBD1 domain will determine whether the ΔF_{508} CF mutation is present in $CFTR_{cardiac}$. RT-PCR employing several other primer pairs demonstrates the expression of $CFTR_{cardiac}$ in normal human atrium and CF atrium and ventricle. Electrophysiological studies of myocytes isolated from normal human atria demonstrate that elevation of cAMP elicits time-independent Cl^- currents.(Supported by HL-30143, AHA and AHA Nevada Affiliate).

Tu-PM-B5

EXTRACELLULAR ATP ACTIVATES A Cl^- CONDUCTANCE IN MOUSE VENTRICLE
((Paul C. Levesque and Joseph R. Hume)) University of Nevada School of Medicine, Reno NV, 89557.

The potent and diverse effects of extracellular ATP on cardiac muscle contractility have been attributed in part to purinoceptor linked activation of K^+, Ca^{2+} and non-specific cation conductances. After pharmacologically eliminating possible interfering currents due to activation of these channels, extracellular ATP (100 μM) elicited a time-independent background conductance in voltage-clamped ventricular myocytes enzymatically dissociated from mouse heart. ATP activated the conductance during voltage steps ranging from +40 to -110 mV from a holding potential of -30 mV within 1-2 min in 7 of 16 cells. The reversal potential for the conductance was -30±2.9 mV (predicted E_{Cl} -31.5 mV). Partially substituting external Cl^- with aspartate attenuated the ATP-activated currents and shifted the reversal potential to values close to those predicted for E_{Cl} (n=4), suggesting the Cl^--selective nature of the conductance. The poorly hydrolyzable ATP analog, ATPγS (100 μM), elicited the time-independent conductance in 40% of cells tested (compared to 46% using ATP) suggesting the involvement of a purinoceptor in activation of the conductance rather than a mechanism involving hydrolysis of ATP. Preliminary data indicates that the conductance may be mediated via P_2- and not P_1-purinoceptor stimulation since the P_1-purinoceptor agonist adenosine (500 μM) had no effect in 7 cells. Activation of the conductance by ATP is not likely dependent on increased $[Ca^{2+}]_i$ since the percentage of cells in which ATP activated the current was similar in cells dialyzed with or without 10 mM EGTA. The results suggest that ATP activates a Cl^- conductance in mouse ventricular myocytes through stimulation of a P_2-purinoceptor. An ATP-activated Cl^- conductance could be of physiological and pathophysiological significance considering the ability of Cl^- channels to modulate cardiac electrical activity and the fact that ATP may be an important neuromediator in the heart. (Supported by NIH grant HL 30143 and HL 08505)

Tu-PM-B6

PARTIAL LOCALIZATION OF THE ANION PERMEATION PATHWAY IN CFTR. ((S. McDonough, N. Davidson, H.A. Lester, N.A. McCarty)) Div. of Biology, Caltech, Pasadena, CA, 91125. (Spon. by S. Benzer)

The cystic fibrosis transmembrane conductance regulator (CFTR) is a chloride channel member of the ATP-binding cassette superfamily, consisting of twelve putative membrane spanning domains, two nucleotide binding folds, and a regulatory (R) domain. Predictions of which parts of CFTR form the permeation pathway and determine chloride selectivity have been complicated by this transporter-like topology and by the lack of homology among different chloride channels. In a previous paper (*J. Gen. Physiol.* 102: 1-23, 1993), we showed that diphenylamine-2-carboxylic acid (DPC) is an open-channel blocker of CFTR expressed in *Xenopus* oocytes. Here we use site-directed mutagenesis to study residues in transmembrane domains (TM) 6,11, and 12 corresponding to the electrical binding distance of DPC. When mutated, these residues alter the affinity of the channel for DPC and give altered unblocked current properties, showing that these domains at least line the pore. Mutations in TM-6 gave varying degrees of outward, rather than inward, rectification, and one mutation in TM-11 gave voltage-dependent current relaxations. DPC blocked all mutants at hyperpolarized, not depolarized, potentials. Analysis of the geometry of the DPC molecule allows us to propose that TM-6 and TM-12 are alpha-helical. These results may guide elucidation of the structure-function relations of other chloride channels and members of the ABC superfamily. (Support: NIH, CFF)

Tu-PM-B7

VOLUME-ACTIVATED CHLORIDE CHANNELS IN DRUG-SENSITIVE AND -RESISTANT CELL LINES. ((G.R. Ehring, Y.V. Osipchuk, M.D. Cahalan)) Department of Physiology and Biophysics, University of California, Irvine CA, 92717.

The *MDR1* gene product, P-glycoprotein, produces the multiple drug-resistant phenotype by transporting a broad class of hydrophobic molecules out of the cell. In addition to transporting chemotherapeutic agents, it has been proposed that P-glycoprotein forms a volume-activated chloride channel (Valverde et al. 1992. Nature 355:830). We examined rhodamine 123 efflux (as a measure of drug transport function) and volume-activated chloride currents in two pairs of drug-sensitive and -resistant cell lines. Western Blotting, FACS analysis, and high rates of rhodamine efflux confirmed expression and function of P-glycoprotein in the doxorubicin-resistant cell line, 8226-Dox_{40}, and in *MDR1*- transfected NIH-3T3 fibroblasts, but not in doxorubicin-sensitive 8226 myeloma cells or in control NIH-3T3 cells. During whole-cell patch clamp experiments, cell swelling was achieved either by dialysis of cytoplasm using hypertonic pipette solution or by bath solution exchange to hypotonic solution. With either technique, osmotic challenge resulted in large outwardly rectifying chloride currents of similar magnitude and properties in the control and corresponding drug-resistant cell line. Thus the activity of volume-activated chloride currents is independent of the expression of P-glycoprotein and drug efflux. Supported by NIH NS14609.

Cell Type	g_{Cl} (nS)	Efflux Rate (s^{-1})
3T3-Control	27.7 ± 12 (n = 14)	< 0.1 x 10^{-3} (n= 75)
3T3-MDR	31.5 ± 12 (n = 33)	2.4 ± 0.5 x 10^{-3} (n= 54)
8226-Control	6.1 ± 3.8 (n = 12)	< 0.1 x 10^{-3} (n= 32)
8226-Dox_{40}	7.7 ± 5.3 (n = 10)	2.1 ± 0.7 x 10^{-3} (n= 44)

Tu-PM-B8

PHARMACOLOGICAL SENSITIVITIES OF VOLUME-ACTIVATED CHLORIDE CONDUCTANCE AND RHODAMINE 123 EFFLUX IN DRUG-SENSITIVE AND -RESISTANT CELL LINES. ((Y.V. Osipchuk, G.R. Ehring, and M.D. Cahalan)) Department of Physiology and Biophysics, University of California, Irvine CA, 92717.

P-glycoprotein has been proposed to function as a drug-efflux pump and as a volume-activated chloride channel. In patch-clamp experiments reported in the accompanying abstract, similar levels of volume-activated chloride conductance (g_{Cl}) were observed in drug-sensitive and -resistant cells. Here, we compare the ability of DIDS, NPPB, and verapamil to block g_{Cl} or rhodamine efflux (as a measure of P-glycoprotein's drug efflux function). Verapamil is a potent inhibitor of rhodamine 123 efflux (K_i of 0.3 μM). In contrast, 10 μM verapamil had no effect on g_{Cl} measured either by patch clamp or by SPQ imaging of intact cells. On the other hand, DIDS and NPPB blocked g_{Cl} with potencies (K_i < 100 μM for NPPB, < 1 mM for DIDS) that were similar in patch-clamp and SPQ imaging experiments. Neither DIDS nor NPPB influenced drug efflux at doses that blocked g_{Cl}. Furthermore, the presence of doxorubicin or vincristine (200 μM) in the patch pipette had no influence on g_{Cl} at concentrations at which transport via P-glycoprotein occurs in intact drug-resistant cells; dialysis of doxorubicin was confirmed directly by fluorescence measurements. Thus, pharmacological agents differentially block drug efflux and g_{Cl}. Supported by NIH14609

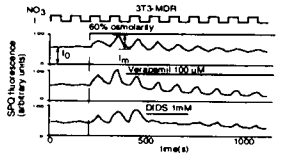

Repetitive quenching/unquenching of SPQ fluorescence by I/NO_3 perfusion as an assay for volume activated g_{Cl} in intact cells.

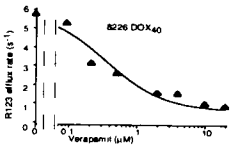

Dose-response curve for verapamil inhibition of R123 efflux in drug resistant cells.

Tu-PM-B9

CHLORIDE CURRENTS IN MAMMALIAN SKELETAL MUSCLE FIBERS MEASURED WITH A VASELINE GAP TECHNIQUE ((Ch. Fahlke, T. Hiller and R. Rüdel)) Department of General Physiology, University of Ulm, D-89069 Ulm (Spon. by P. Fromherz)

Cl^- currents were measured in segments of adult rat *psoas major* fibers mounted in a chamber with 2 vaseline seals. Na^+ and K^+ currents were avoided by using TEA as the major cation in the external and internal solutions (pH 7.4; 300 mosmol/l). The holding potential was -85 mV. Cycles of test steps varying between -125 and +45 mV yielded currents showing deactivation immediately upon hyperpolarization and activation upon depolarization. The activation, when fitted with the sum of 2 exponentials, yielded a smaller time constant changing from 76.1 ms at +55 mV to 231 ms at -45 V, and a larger, potential-independent time constant (457 ms). The steady-state activation curve was described by a single Boltzmann distribution with a half-maximal activation at -38 mV and a slope of 1/15.4 mV at the inflexion point. At negative potentials a potential-dependent deactivation with 2 time constants between 29.6 ms and 115.6 ms at -105 mV and 48.3 ms and 213.9 ms at -55 mV was observed. Varying a 15-s prepulse potential, the instantaneous current at a constant test potential decreased at positive potentials indicating an inactivation process. All kinetic parameters were not affected by variation of $[Cl^-]_i$. These currents should be responsible for the large g_{Cl} of skeletal muscle fibers as they were blocked by 0.1 mM 9-AC and the halogen selectivity was Cl>Br>I. Supported by DFG Ru 138-17/3.

Tu-PM-B10

PURIFICATION AND FUNCTIONAL RECONSTITUTION OF A VOLTAGE-GATED CHLORIDE CHANNEL FROM *TORPEDO* ELECTRIC ORGAN ((R.E. Middleton, D.J. Pheasant and C. Miller)) HHMI, Dept. of Biochemistry Brandeis University, Waltham, MA

The electric organs from *Torpedo* rays contain an unusual voltage-gated Cl^- channel that has two identical and independently gated Cl^- conducting pathways. This channel was previously expression-cloned in oocytes (ClC-0, Jentsch et. al., 1990). In order to study the structural foundation for this "double-barreled" channel, we have purified this protein from a CHAPS extract of electric organ membranes. We used an immunoaffinity column made with purified polyclonal antibodies specific to an 18-residue epitope beginning at Glu-642 of ClC-0. The purified Cl^- channel was shown to be a single band of ~ 80 kDa by SDS-PAGE and was enriched about 15-fold, consistent with its high abundance in electrocytes. Digestion with either endoglycosidase H or N-glycanase increased the mobility ~2 kDa. The purified protein, when reconstituted into liposomes, was shown to be active by ^{36}Cl flux; fusion of these liposomes into planar lipid bilayers revealed fully functional "double-barreled" Cl^- channels. These results demonstrate that the Cl^- channel is built from this one glycosylated polypeptide. The size of the CHAPS-solubilized channel was estimated by sedimentation in sucrose density gradients, using the acetylcholine receptor (~600 kDa dimer, ~300 kDa monomer) and the Na/K-ATPase (~150 kDa) as standards. The channel's apparent molecular weight is 150-200 kDa. Therefore, the "double-barreled" Cl^- channel is most likely constructed as a homodimer.

K CHANNELS II

Tu-PM-C1

CHARACTERIZATION OF A NOVEL FAMILY OF INWARD RECTIFIER-LIKE POTASSIUM CHANNEL SUBUNITS. ((C.T. Bond, M.P. Kavanaugh, J.P. Adelman)) Vollum Institute for Advanced Biomedical Research Oregon Health Sciences University, Portland, OR 97201

Two distinct subtypes of inwardly rectifying potassium channels have recently been described, those in which the conductance properties are modulated primarily by voltage-dependent removal of intracellular Mg^{2+} block, and those which are in addition modulated by G-proteins. Structurally these channels share a common architecture, and retain the pore sequence found in voltage-dependent potassium channels. We have developed a novel PCR strategy which relies on a limited number of conserved residues in the pore region of potassium channels as the sole specificity determinants. Using this approach, we isolated 8 new members of this family from rat heart, skeletal muscle and brain. The mRNAs encoding these subunits are differentially expressed, some restricted to specific brain regions, while others are found in many CNS and peripheral tissues, including some areas which are not known to contain inwardly rectifying potassium conductances. Injection of *Xenopus* oocytes with RNA transcribed from one member of this family, BIR-10, resulted in the expression of inwardly rectifying potassium currents. These currents were sensitive to a voltage-dependent block by external sodium and calcium ions; external Ba^{2+} also produced a voltage-dependent block ($I.C._{50}$ = 3 μM; 90 mM external K+ at -90 mV). The currents were insensitive to TEA. Using the cut-open oocyte recording configuration, the relief of internal Mg^{2+} block by hyperpolarizing voltage pulses could be observed as a rising phase in the current traces within the initial 1 ms. The time constants of activation as a function of voltage yielded a bell-shaped curve with a peak of ~300 μs, consistent with a model in which the channel alternates between the blocked and unblocked states (Mg^{2+}Cblocked <---> Mg^{2+} + Cunblocked). Fitting the data to a model incorporating voltage-dependent rate constants for block and unblock suggests that the internal Mg^{2+} site within the conduction pathway senses approximately 20% of the electric field.

Tu-PM-C2

POST-TRANSCRIPTIONAL AND TRANSLATIONAL REGULATION OF THE RAPIDLY INACTIVATING K^+ CHANNEL GENE, KV1.4. ((R. Wymore, K. Kinoshita, J. Aiyar, G. Gutman, K. G. Chandy)) Dept. of Physiology & Biophysics, and Dept. of Microbiology & Molecular Genetics, University of California, Irvine, CA 92717

The cardiac K^+ channel gene, Kv1.4, gives rise to three transcripts ranging in size from 2.4-4.5 kb. In order to characterize the organization of this gene we have isolated a mouse genomic Kv1.4 clone. Alignment of the mouse genomic sequence with that of hKv1.4 (HPCN2) cDNA shows the presence of a 3.4 kb intron 890 bp upstream of the start of translation. One region of approximately 280 bp upstream, and another of ~3400 bp (which includes the entire ~2 kb protein coding region) downstream of this site, are each contiguous in the genome. The sequenced genomic region accounts for essentially all of the 4.5 kb mRNA, although the precise ends of this transcript have not been defined. The 3'-untranslated region (UTR) contains several AUUUA and AUUUG motifs which are thought to destabilize mRNAs, and these are also present in rat, bovine and human Kv1.4 cDNAs. It also contains three conserved polyadenylation signals, alternate utilization of which could generate mRNAs of differing stabilities. Consistent with this idea, injection into *Xenopus* oocytes of a truncated mKv1.4 cRNA lacking the AUUUA motifs leads to an average of 40-60 μA of current, while injection of cRNA containing the AUUUA motifs results in at least a 5-fold decrease in channel expression. The 5'-UTR of mKv1.4 may also serve to regulate channel expression. This region is ~85% identical to hKv1.4, and contains 8 consensus translation start sites ([G,A]NNATG) which, based on the 5'-3' scanning model, would lead to a lowering of translational efficiency. The shortest Kv1.4 transcript (2.4 kb, including the ~2 kb coding sequence) can contain at most 400 bp of UTR, and should lack the 3'-AUUUAs and most of the 5'-ATGs. This transcript might therefore exhibit increased stability and translational efficiency. (Supported by grants from the NIH [AI-24783] and from Pfizer Inc.)

Tu-PM-C3

NON-STATIONARY FLUCTUATION ANALYSIS OF DELAYED K^+ CURRENT IN GUINEA PIG SINO-ATRIAL NODE AND TRANSFECTED HEK-293 CELLS. ((L.C. Freeman and R.S. Kass)) University of Rochester School of Medicine, Rochester, NY 14642.

The non-inactivating component of delayed rectification in guinea pig (GP) heart (I_{Ks}) has been associated with the activity of densely clustered low conductance channels. Attempts to resolve single channel openings of I_{Ks} in membrane patches isolated from either native heart cells or *Xenopus* oocytes which express the underlying minK channel have been unsuccessful, presumably because of a high density of small conductance channels. Resolution of current fluctuations in whole cell recordings of GP ventricular I_{Ks} have been limited by the large number of channels present in the large (100 pf) myocytes. Here, we report the measurement and non-stationary noise analysis of time and voltage-dependent fluctuations in membrane currents recorded from smaller (10 pf) cells: native heart cells from GP sino-atrial node (SAN) and HEK-293 cells transiently transfected with minK. I_{Ks} channels were activated by 1.5 to 2 second pulses from -40 mV holding potential (h.p.) to positive test potentials (+60 to + 100 mV). Fluctuation analysis was performed using either time-dependent currents activated during the test pulse or tail currents recorded on return to the h.p. Local averages of 4-16 records were computed and subtracted from individual records to measure variance. The measured fluctuations were diminished during pharmacological blockade of I_{Ks}, and undetectable during pulses to voltages at which I_{Ks} is not appreciably activated. For current fluctuations measured at +60 mV but not -20 mV, the variance (Var) of the macroscopic current could be described as a function of the mean current (I) with initial slope equal to the single channel current (i) : $\langle Var \rangle = Ii - I^2/N$. The relationship between <I> and <Var> was generally linear rather than parabolic, consistent with a large number of channels even in these cells. Single channel unitary currents estimated at +60 mV in 0.5 mM external K^+ at room temperature were 0.24 pA and 1.55 pA for I_{Ks} in SAN and HEK-293 cells, respectively.

Tu-PM-C4

I_{sK} EXPRESSED IN *XENOPUS LAEVIS* OOCYTES IS CONTAMINATED BY AN ENDOGENOUS CONDUCTANCE.
((H.S. Yeh, S.M. Taffet, M. Delmar and J.M.B. Anumonwo)). SUNY/Health Science Center, Syracuse NY 13210. (Spon. by M. Delmar).

Xenopus oocytes have a calcium-dependent chloride conductance which is sensitive to Mn^{2+}. The current is considered small relative to currents from expressed exogenous channels. We have carried out experiments in non-injected and in mRNA injected (40 ng/nl mRNA for murine I_{sK}) oocytes using the two electrode voltage clamp technique in Barth's solution. Whole cell recordings were done 36-48 hours post injection for mRNA injected oocytes. Voltage clamp protocol consisted of 5 or 10 sec depolarizing pulses to a maximum of +50 mV from a holding potential (HP) = -80 mV and tail currents were recorded at -40 mV. Endogenous tail current amplitudes in non-injected oocytes averaged -327.3 nA ± 147 (X ± SEM, n=6) after a pulse to +40 mV. Mn^{2+} (1 mM) reversibly abolished the large inward tails (n=4). In mRNA injected oocytes, tail currents averaged 906.8 nA ± 146 (X ± SEM,n=6) in control. Figure shows Mn^{2+} effect of increasing outward tail current amplitude in an mRNA injected oocyte. Current traces are in the absence (panel A) and presence (panel B) of 1 mM Mn^{2+}. In another set of four mRNA injected oocytes, 1 mM Mn^{2+} caused a 10 mV shift towards the theoretical reversal potential for tail currents. These results suggest that the Mn^{2+}-sensitive endogenous conductance contaminates I_{sK} expressed in oocytes, and must be taken into consideration in any analysis of the exogenous I_{sK}.

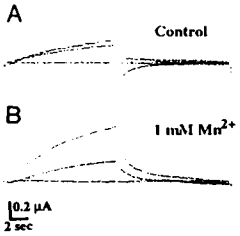

Tu-PM-C5

INTRACELLULAR ACIDIFICATION INHIBITS MURINE I_{sK}
((H.S. Yeh, G.E. Morley, S.M. Taffet, M. Delmar and J.M.B. Anumonwo)). SUNY/Health Science Center, Syracuse NY 13210. (Spon. by G.E. Morley).

The effect of intracellular acidification on the slowly activating potassium current (I_{sK}) was determined in *Xenopus* oocytes (n=6) injected with 40 ng/nl murine I_{sK} mRNA. Whole cell recordings were done 36-48 hours post injection. The voltage clamp protocol consisted of 5 or 10 sec depolarizing pulses to a maximum of +50 mV from a holding potential (HP) = -80 mV; tail currents were recorded at -40 mV. pHi was optically recorded using a pH-sensitive fluorescent dye, seminaphthorhodafluor-1, (dextran, SNARF). Acidification was achieved using either Na acetate Barth's solution balanced at pH 6.8 or normal Barth's solution saturated with 100% CO_2. Figure shows time course of intracellular acidification (horizontal bar) effect on the I_{sK}; HP=-40, test pulse +30 mV every minute. Continuous line indicates changes in fluorescence ratios (right Y-axis); filled circles indicate amplitude of I_{sK} (left Y-axis). Intracellular acidification was closely followed by a drop in amplitude of I_{sK}. Both pHi and I_{sK} recovered upon washout. In four oocytes, acidification (pHi= 6.4-6.75) caused a 50% reduction of I_{sK} at all membrane potential tested. Normalized isochronal (10-sec) activation plots were fitted using the Boltzman function. Current kinetics were not affected by intracellular acidification (n=3); V_h and slope factor were respectively +4.18 mV and 14.6 (pH=7.4) and +5.83 mV and 16.98 (pH= 6.8). These data suggest that the I_{sK} is very sensitive to intracellular proton concentration.

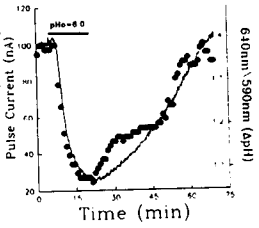

Tu-PM-C6

INTRACELLULAR H^+ STRONGLY INHIBITS ROMK1 K^+ CURRENT EXPRESSED IN *XENOPUS OOCYTES*
T.D. Tsai, M.E. Shuck*, D.P. Thompson*, M.J. Bienkowski* and K.S. Lee. Cardiovascular Diseases Research, * Cell Biology and *Parasitology. The Upjohn Laboratories, Kalamazoo, MI 49007

Intracellular pH was measured in *Xenopus oocytes* injected with rat kidney ROMK1 cRNA. Concomitant pH and current recordings were made using pH-sensitive microelectrode and the two-microelectrode voltage clamp technique. Oocytes injected with ROMK1 (45 ng/oocyte) had hyperpolarized resting potential of -98.7±0.98 mV (n=15) compared to -50.1±3.27 mV (n=12) of the water injected. At 0 mV holding potential in 100 mM external K^+, step pulses elicited a slightly inward-rectifying K^+ current that was inhibited by <1 mM Ba^{2+}. Lowering of intracellular pH to within the normal physiological range (7.2 to 6.54), using acetate-buffered 100 mM K^+ solution, strongly reduced the ROMK1 current. The relationship between ROMK1 slope conductance near the reversal potential and intracellular pH between 7.2 and 6.54 could be fitted by a titration curve for the binding of four H^+ ions to a site with pK_a of -6.92. The H^+ blockade of ROMK1 currents did not alter current activation kinetics or show voltage dependence. In constrast, extracellular pH reduction from 7.4 to 6.0 using biphthalate-buffered 100 mM K^+ solution produced no consistent reduction of the ROMK1 current. The high sensitivity of the ROMK1 channel to intracellular pH is similar to that reported for the native small-conductance K^+ channel in apical membrane of rat cortical collecting tubule and that of the luminal K^+ channel of thick ascending limb of Henle's loop. Thus, the unique sensitivity of the kidney channels to intracellular pH is preserved in the ROMK1 channel expressed in *Xenopus oocytes*.

Tu-PM-C7

POINT MUTATION ENHANCES SENSITIVITY TO ETHANOL IN A HUMAN K^+ CHANNEL. ((T.B. Vyas[1], C. Choe[1], A. Wei[2] and M. Covarrubias[1])). 1) Jefferson Medical College, Philadelphia, PA 19107 and 2) Washington University School of Medicine, St. Louis, MO 63110.

Ethanol (EtOH) at low concentrations (17-170 mM) selectively blocks *Drosophila Shaw*2 K^+ channels expressed in *Xenopus* oocytes (*Proc. Natl. Acad. Sci. USA 90*:6957-6960, 1993). It mainly reduced *Shaw*2 macroscopic currents and slowed down their rising phase. It also reversibly reduced the mean open time of single channel currents (0.82 ms and 0.64 ms, control and EtOH-treated, respectively) with no change in single channel conductance. By contrast, EtOH minimally affected a human *Shaw* homologue (*hKv3.4*). Sequence analysis revealed a unique hydrophobic amino acid within the S4-S5 linker (Ile^{319}) in *Drosophila Shaw*2. The equivalent position is occupied by Gly in all EtOH insensitive K^+ channels. Mutation of Gly^{371} to Ile^{371} in human *Shaw* K^+ channels significantly enhanced sensitivity to 170 mM EtOH by ~3.5-fold. The fraction unblocked peak current was: 0.96±0.01 in WT (n=4) and 0.86±0.03 in G371I (n=4). These results strongly support the protein hypothesis of EtOH action. Supported by NIAAA.

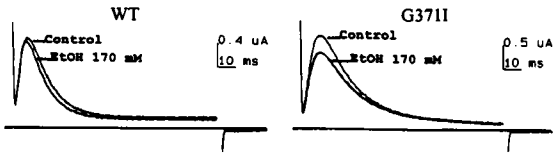

Tu-PM-C8

QUATERNARY QUINIDINE DERIVATIVES AS A TOOL TO STUDY BLOCK OF HUMAN POTASSIUM CHANNELS. ((T.C. Rich, S.N. Yeola, I.A. Blair, S.W. Yeola and D.J. Snyders)) Departments of Biomedical Engineering, Medicine and Pharmacology, Vanderbilt University, Nashville, TN.

We have previously reported that quinidine inhibits the human atrial delayed rectifier hKv1.5 by acting as a open channel blocker. To test the proposal that this action is mediated by the charged form of quinidine, we synthesized N-alkyl derivatives of quinidine. Alkyl iodides of different carbon chain length (n=1-7) were used to react with the quinuclidine nitrogen of quinidine to form the corresponding quinidinium salts (CnQ^+). The chemical structure and purity of the reaction products were confirmed by ^{1}H-NMR and mass spectrometry. Their effect on hKv1.5 currents was studied in whole cell voltage clamp mode using a stably expressing clonal L-cell line. Extracellular application of 20 µM $C1Q^+$ failed to reduce hKv1.5 current. With 20-50 µM added to the intracellular (pipette) solution, typical time-dependent relaxation of the current was observed, resulting in >70% block at +50 mV. In contrast, $C5Q^+$ and $C7Q^+$ were active when applied from the extracellular side, but it required ≥ 20 min to reach steady-state conditions (69% block for 20 µM $C7Q^+$), which is ~3 times slower than quinidine. The similarity of the action of intracellular $C1Q^+$ to that of quinidine and the slow onset of the effect of long chain quinidiniums indicate that the cationic form of quinidine blocks the hKv1.5 pore from the inside. Supported by NIH grants GM08452, GM31304, HL46681 and HL47599.

Tu-PM-C9

CHARACTERIZATION OF THE ATP-INHIBITED K⁺ CURRENT IN CANINE CORONARY SMOOTH MUSCLE CELLS

X. Xu and K.S. Lee. Cardiovascular Diseases Research, Upjohn Laboratories, Kalamazoo, MI 49007.

Intracellular ATP inhibited K^+ currents (K_{ATP}) in canine coronary artery smooth muscle cells were characterized in whole cell configuration using the suction pipette method. Cells dialyzed internally with solutions containing 5 mM ATP (ATP_i) showed little detectable whole cell currents negative to -30 mV. However, cells dialyzed with ATP_i-free solutions developed a time and voltage independent current, reaching a maximum of 132 ± 25 pA at -40 mV in 10 min following patch rupture. After "run-up", the current showed little "run-down". Concentration dependent inhibition by ATP_i yielded a K_i of 350 μM and Hill coefficient of 2.3. In ATP_i-free solutions, the large current at -40 mV was reduced by glyburide with a K_i of 20 nM and a Hill coefficient of 0.95. In 1 mM ATP_i solutions, the small current at -40 mV was increased by P-1075 from 8 ± 2 pA to 143 ± 33 pA, with a K_d of 0.16 μM and a Hill coefficient of 1.7. The effect of P-1075 was antagonized by glyburide. Maximal inducible current density at -40 mV by either ATP_i depletion or addition of P-1075 was similar, at 3.6 ± 0.6 pA/pF and 3.4 ± 0.6 pA/pF respectively. External Ca^{2+} had no effect on this current. Finally, 20 and 50 μM adenosine increased the current slope conductance between -90 to -40 mV in 1 mM ATP_i by 36 ± 15 % and 73 ± 10 %, respectively. The K_{ATP} current, although very small in these cells, was extremely effective in causing membrane potential hyperpolarization.

Tu-PM-C10

ACTIVATION OF INWARD-RECTIFIER K⁺ CHANNELS (K_{IR}) DILATE SMALL CEREBRAL AND CORONARY ARTERIES IN RESPONSE TO ELEVATED POTASSIUM.

((Harry J. Knot, Paul A. Zimmermann* and Mark T. Nelson)) University of Vermont, Depts. of Pharmacology and *Cardiology, CMRF, 55A South Park Drive, Colchester VT 05446-2500.

Potassium release from active neurons and cardiac muscle may be sufficient to cause arterial dilation through activation of inward rectifier potassium (K_{IR}) channels. This may be a factor linking neuronal and cardiac metabolism to blood flow. We have recently characterized the properties of K_{IR} currents in smooth muscle cells isolated from resistance-sized cerebral (Quayle et al. (1993) Am. J. Physiol.265 (Cell Physiol.34)) and coronary (see abstract by Bonev, Robertson & Nelson this meeting) arteries. K_{IR} currents in these tissues were blocked by low concentrations of Ba^{2+} (1-10 μM external Ba^{2+} at -60 to -40 mV). We tested the hypothesis that elevated extracellular potassium dilates these arteries by activating inward-rectifier K^+ channels.We used intact isolated pressurized (60 mm Hg) resistance-sized rat posterior-cerebral (mean diameter: 107 ± 36 μm, n = 31) and coronary (septal) (mean diameter: 118 ± 31 μm, n = 44) arteries that develop myogenic tone in response to pressure. Elevated extracellular K^+ (K^+_o) (7.5-20 mM) fully dilated these arteries. Higher concentrations of K^+ (25-35 mM) gave sustained constrictions. Low concentrations of barium (half block = 7 μM) completely blocked the vasodilator part of the response to elevated K^+. Elevating K^+ from 5 to 15 mM hyperpolarized isolated cerebral arteries by 11±5 mV (n=3). The hyperpolarization was blocked by 30 μM Ba^{2+}. The vasodilator effect of elevated K^+ was seen in the absence of the endothelium and was not blocked by glibenclamide (10 μM), 4-Aminopyridine (1 mM) and TEA⁺ (1 mM). The vasodilation was unaffected by α, β, serotonergic, histaminergic and muscarinic receptor blockers. We, therefore, propose that increasing K^+_o activates K_{IR} channels causing membrane hyperpolarization which leads to coronary and cerebral artery dilation. These channels may play an important physiological role in the (auto)regulation of blood flow in brain and heart and may be important during cerebral and cardiac ischemia.

HJK is a Fellow of the AHA Vermont affiliate. Supported by the NSF and NIH.

EXOCYTOSIS AND ENDOCYTOSIS

Tu-PM-D1

ANNEXIN IV REDUCES THE RATE OF LATERAL LIPID DIFFUSION WHEN IT BINDS TO NEGATIVELY CHARGED LIPID BILAYERS IN THE PRESENCE OF CALCIUM

((R. Gilmanshin, C.E. Creutz[1]) and L.K. Tamm)) Dept. of Molecular Physiology and Biological Physics and Dept. of Pharmacology[1], University of Virginia School of Medicine, Charlottesville, VA 22908

Bovine annexin IV (endonexin) that was expressed in *E. coli* was bound to supported planar bilayers composed of 1-palmitoyl-2-oleoyl-phosphatidylcholine (POPC) in the first monolayer facing the substrate, and varying mole fractions of POPC, 1-palmitoyl-2-oleoyl-phosphatidylglycerol (POPG), and small amounts of the fluorescent lipid analogs NBD-PC or NBD-PG in the second monolayer facing the large aqueous compartment. Lateral diffusion coefficients and mobile fractions of these phospholipids were measured by fluorescence recovery after photobleaching (FRAP) as a function of protein concentration and lipid composition in the presence of 2 mM $CaCl_2$ or 1 mM EDTA. In the absence of annexin IV, the lateral diffusion coefficients depended only weakly on the POPC:POPG ratios and were 3.0 $\mu m^2/s$ for NBD-PG (no Ca^{2+}), 2.5 $\mu m^2/s$ NBD-PG (2 mM Ca^{2+}), and 1.8 $\mu m^2/s$ for NBD-PC (with or without 2 mM Ca^{2+}). In the presence of 2 mM Ca^{2+} these diffusion coefficients decreased as a function of the added annexin concentration. A sigmoidal transition from a state with "rapid" lipid diffusion to a state with "slow" lipid diffusion occurred at about 80 nM annexin IV and independent of the POPC:POPG ratio. However, the magnitude of the decrease of the lipid lateral diffusion coefficients depended strongly on the amount of POPG in the membrane, ranging from a 1.6 fold decrease at 10 mol % POPG to a 25 fold decrease at 84 mol % POPG. Since similar results were obtained with the NBD-PG and NBD-PC lipid probes, it is concluded that annexin IV changes the fluid phase properties of these membranes in a Ca^{2+}- and POPG-dependent fashion rather than forming long-lived stoichiometric complexes with the POPG molecules.

Tu-PM-D2

MONOLAYER AND COMPLETE FUSION STAGES OF THE LIPOSOME - PLANAR LIPID BILAYER INTERACTION DISSECTED BY MODULATION OF MEMBRANE LIPID COMPOSITION.

((L.V. Chernomordik, A.N. Chanturiya, J. Green & J. Zimmerberg)) LTPB, NICHD, NIH, Bethesda, MD 20892

We used a liposome-planar bilayer lipid membrane (BLM) fusion model to test a hypothesis for the mechanism of membrane fusion involving the formation of a highly bent intermediate between membranes - - the fusion stalk. This 'stalk' hypothesis invokes two successive local bending deformations of membrane monolayers in opposite directions during fusion to 1) connect the contacting membrane monolayers (monolayer fusion) and, then, 2) break distal monolayers to form a fusion pore (complete fusion). Since the lipid monolayer propensity to bend reflects the effective molecular shape of lipids, the stalk model gives specific predictions on how modulation of lipid composition should affect membrane fusion. Two assays: conductance measurements and fluorescence microscopy were used to distinguish monolayer fusion from complete fusion for decane-containing BLM with liposomes containing porin ion channels and fluorescent lipid at a self-quenching concentration. We found that the incorporation of inverted cone-shaped lysophosphatidylcholine (LPC) into the contacting monolayers of membranes caused potent inhibition of monolayer fusion. No inhibition was observed when arachidonic acid (AA), having the opposite molecular shape to LPC, was used in similar experiments. Addition of LPC to modify the distal monolayer of the BLM also had no effect on monolayer fusion but promoted complete fusion. In contrast, modification of the BLM distal monolayer by AA resulted in a dramatic inhibition of complete fusion. These results are consistent with the stalk model.

Tu-PM-D3

G-PROTEIN INHIBITORY CONTROL OF A K⁺-SELECTIVE CHANNEL OF LARGE CONDUCTANCE PRESENT IN ADRENAL CHROMAFFIN GRANULE MEMBRANES

(N. Arispe, P. De Mazancourt* and E. Rojas) LCBG, MPB, NIDDK, NIH, Bethesda, MD 20892.

We have previously reported (J. Membrane Biol. 130: 191-202, 1992) that, by allowing intact adrenal chromaffin granules to fuse with acidic phospholipid planar bilayer membranes, we detected the presence of a K^+-selective channel (CG-type K^+-channel) of large conductance (150-300 pS depending on $[K^+]$). Based on these properties we proposed that the role of this channel may include ion and catecholamine movements during granule assembly and recycling. We now report that the activity of the CG-type K^+-channel is controlled by a mechanism involving inhibitory guanine nucleotide binding proteins (G-proteins). Using antibodies against specific α subunit sequences of the G protein, immunoblot analysis identified the presence of G_o, G_i and G_3 but not G_q in a highly purified preparation of adrenal chromaffin granules. Furthermore, functional analysis of CG-type K^+-channel incorporated into bilayer membranes showed that the nonhydrolyzable analogs GDPβS and GTPγS have opposite effects on channel activity, GDPβS profoundly increasing and GTPγS reducing the open probability p_o. Furthermore, application of the antibodies used in the immunoblot analysis to the cytosolic side of the channel activated the CG-type K^+-channel and reverted in part the blockade by GTPγS or NaF (20 mM). We concluded that the activity of the chromaffin granule K^+-channel of large conductance is kept under tight control by direct action of G-proteins on the channel.

Tu-PM-D4

CHLORIDE CHANNELS IN MAST CELLS: BLOCK BY DIDS AND ROLE IN EXOCYTOSIS.

((M. Lindau and J. Dietrich)) MPI for Medical Research, D-69120 Heidelberg and Schering AG, D-13342 Berlin. (Spon. by W. Almers)

In rat mast cells we investigated the influence of DIDS and of extracellular $[Cl^-]$ on the Cl^- current induced by intracellular cyclic AMP and on hexosaminidase secretion from intact cells stimulated with compound 48/80. Inhibition of the Cl^- current by extracellular DIDS is voltage and time-dependent. Steady state current at +70 mV is blocked with IC_{50}=2.3 μM. The number of open channels at -10 mV is reduced with IC_{50}=22 μM. Upon depolarization from -10 to +70 mV the outward current diminishes with millisecond kinetics. Steady state current and time constant both decrease with increasing [DIDS]. DIDS also inhibits exocytosis. With 10 μg/ml compound 48/80 secretion is inhibited with an IC_{50}=50 μM and Hill coefficient n=10. At half optimal stimulation with 1 μg/ml inhibition occurs with IC_{50}=10 μM, n=1. The substitution of extracellular Cl^- by glutamate has very small effects on secretion stimulated with 10 μg/ml compound 48/80. We conclude that the Cl^- current is not essential for exocytosis but may enhance secretion at suboptimal stimulation. Supported by DFG (Sfb 312/B6)

Tu-PM-D5

INCREASED CYTOPLASMIC CALCIUM FACILITATES THE RELEASE OF SECRETORY PRODUCTS AFTER EXOCYTOTIC VESICLE FUSION. ((R. Fernández-Chacón & G. Alvarez de Toledo)). Departamento de Fisiología Médica y Biofísica. Universidad de Sevilla. 41009 Sevilla. SPAIN.

We have simultaneously combined patch-clamp measurements of the cell membrane capacitance and the electrochemical detection of serotonin released during single vesicle exocytosis in peritoneal mast cells. To our surprise, the stepwise increases in the cell membrane capacitance owing to single vesicle fusion, were not inmediately followed by release of serotonin. In contrast, there was a variable delay between the two signals (Fig. A), that followed an exponential distribution when plotted as a frecuency histogram (Fig. B). This delay between fusion and release did not depend on the distance at which a secretory vesicle fuses from the electrochemical detector, however, it was strongly associated with the time taken by the exocytotic fusion pore to complete dilation. The average pore expansion time was reduced to a half when the cells were dialyzed through the patch pipette with a calcium concentration in the micromolar range (1.1 μM) (τ=252.4 ms in ~ 50nM calcium versus τ=137.8ms in high calcium) (Fig. C). The characteristic of the amperometric signals, however, were unchanged at different calcium concentrations, suggesting that the exocytotic fusion pore is directly regulated by cytoplasmic calcium more than the release from the granule matrix. These results demonstrate a novel site of regulation of the exocytotic process.

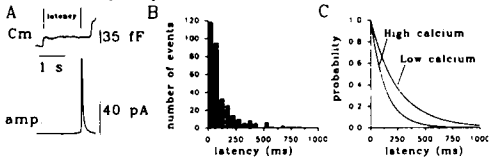

Tu-PM-D6

THE CALCIUM DEPENDENCE OF TRIGGERED EXOCYTOSIS STUDIED USING CAGED CALCIUM: A ROLE FOR GRANULE HETEROGENEITY? ((S.S. Vogel, N.I. Shafi, and J. Zimmerberg)) LTPB, NICHD, NIH Bethesda, MD 20892

Upon fertilization of the sea urchin egg, thousands of pre-docked exocytotic granules fuse with the plasma membrane in response to a rise in intracellular [Ca^{2+}]. Here, we use caged calcium to trigger exocytosis in an *in vitro* preparation of granules and oolemma. Ca^{2+} release was monitored with the fluorescent Ca^{2+} indicator rhod-2 and the fusion reaction with video microscopy and light scattering. UV photolysis of DM-nitrophen (1mM) 50% loaded with Ca^{2+} caused rapid and complete exocytosis. Cytoplasmic proteins and cofactors were not required. Moreover, nitrophen loaded with magnesium, strontium, or barium failed to trigger exocytosis. Granule-plasma membrane fusion begins at random locations across the video field though local cooperativity was observed. The free [Ca^{2+}] observed at the onset of fusion was 13.3±1.3μM, and the range was from 3.6-26.1μM, n=18. Because the appearance of calcium in the medium is controlled by the intensity of UV excitation, we could control the rate of change of [Ca^{2+}]. If we slow the rate of appearance of Ca^{2+}, the threshold for fusion shifts to lower [Ca^{2+}]. The data is easily described by a population of granules with heterogeneous thresholds to calcium and a constant response time of any granule to calcium above threshold. This hypothesis was tested using two subsequent ramps of Ca^{2+}, the first giving only partial fusion. In the second ramp of Ca^{2+}, a higher [Ca^{2+}] (30.6±3.9 μM, n=18) was needed to recruit more granules to fuse. A numerical simulation based on granule heterogeneity simulates our experimental results and its implications for the molecular basis of granule heterogeneity will be discussed.

Tu-PM-D7

EXO-ENDOCYTOSIS AND CLOSING OF THE FISSION PORE IN SINGLE PITUITARY NERVE TERMINALS INTERNALLY PERFUSED WITH HIGH CALCIUM ((M. Lindau and H. Rosenboom)) MPI f. Med. Research, D-69028 Heidelberg and Inst. Neurobiology, Free University, D-14195 Berlin.

When Ca^{2+} is elevated in pituitary nerve terminals by step depolarisation, an instantaneous capacitance increase during the first 80 ms is followed by a slow increase extending over several seconds (Biophys.J. 61:19,1992). We measured capacitance changes associated with exocytosis and endocytosis in single pituitary nerve terminals internally perfused with high Ca^{2+}. At 50 μM Ca^{2+} the capacitance increases by up to 2 %/s which is similar to the slow phase observed during depolarisation. Following exocytosis large downward capacitance steps were measured reflecting endocytosis of large vacuoles. These events were not abrupt but reflected a gradual decrease of fission pore conductance from 8 nS to less than 40 pS during 500 ms. Above 300 pS narrowing of the endocytotic fission pore is ~10 times slower than the previously reported expansion of the exocytotic fusion pore. The transition between 300 pS and 0 pS takes ~200 ms whereas the exocytotic fusion pore measured in mast cells opens from 0 to 280 pS in <100 μs (Spruce et al. Neuron, 4:643,1990). Large intraterminal vacuoles formed in the absence of such endocytic events presumably reflecting granule-granule fusion inside the nerve terminal. Our results indicate that at the site of fusion very high Ca^{2+} is required. At these concentrations granules may fuse with the plasma membrane or among themselves. Furthermore, the properties of the fission pore differ from those of the exocytotic fusion pore reflecting differences between the mechanisms of exocytotic fusion and endocytotic fission.

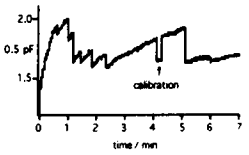

Tu-PM-D8

CALCIUM TRIGGERED EXOCYTOSIS AND ENDOCYTOSIS IN ISOLATED PRESYNAPTIC CELLS.
((T.D. Parsons[1], D. Lenzi[2], W. Almers[1], W.M. Roberts[2])) [1]ZellForschung, Max-Planck-Institute f. Med. For., W69028 Heidelberg, Germany & [2]Institute of Neuroscience, Univ. of Oregon, Eugene, OR 97403

Hair cells of the amphibian sacculus are mechanosensory cells that synapse on to primary afferent axons, utilize small synaptic vesicles, and show calcium-dependent quantal transmission. Exocytosis of synaptic vesicles by hair cells is amenable to study with patch clamp methods because the release sites are located at the cell body. Changes in membrane capacitance that represent exocytosis and subsequent retrieval of plasma membrane were measured (Neher & Marty, 1982). Acutely dissociated hair cells were depolarized from a holding potential of -70 mV to -10 mV for 1 sec, resulting in an average increase in capacitance of 303 $\pm$ 79 fF (n=19). These changes in capacitance correlated with voltage-dependent changes in calcium current, were blocked by external cobalt, and varied linearly with pulse durations ranging from 100 ms to 2 sec. These increases in membrane capacitance were rapidly reversible when perforated patch methods were used for recording, but persisted under whole cell recording conditions. Twenty sec after the stimulus only 22.8 $\pm$ 7.5% (n=7) of the previously exocytosed membrane remained with perforated patch, whereas in whole cell recordings 107.5 $\pm$ 15.1% (n=10) remained. This finding suggests that in hair cells, endocytosis is susceptible to the dialysis of a mobile intracellular factor. The changes in capacitance described here may represent the exocytosis and subsequent retrieval of synaptic vesicle membrane. Supported by HFSPO Fellowship (TDP), NIH grant NS27142 (WMR), and a McKnight Scholars Award (WMR).

Tu-PM-D9

TWO COMPONENTS OF ENDOCYTOSIS IN PRESYNAPTIC TERMINALS.
((G. Matthews and H. von Gersdorff)) Neurobiology, SUNY, Stony Brook, NY 11794.

Membrane retrieval following vesicular exocytosis is a central aspect of vesicle recycling in synaptic terminals. We have used capacitance measurements to monitor the time-course of endocytosis following secretion elicited by Ca current in giant synaptic terminals of goldfish retinal bipolar neurons. A single depolarizing voltage-clamp pulse (arrow in left panel below; duration 250 msec) increased both intraterminal [Ca] and membrane capacitance. Capacitance then recovered rapidly to baseline along an exponential time-course (average τ = 2 ± 0.5 sec). However, after a series of depolarizing pulses (black bar, right panel; 250-msec pulses at 1/sec), which drove [Ca] to higher levels and increased capacitance to a plateau, the recovery of capacitance was much slower (τ = 23 ± 7 sec). This slowing of retrieval following stronger stimulation may represent an important negative feedback mechanism by which the replenishment of vesicle pools, and hence the readiness for continued secretion during sustained stimulation, is regulated in the presynaptic terminal in response to stimulus history.
(Supported by NIH grant EY03821 and NRSA Fellowship EY06506)